

Supplementary Material

Mathematical model

One-dimensional blood flow equations characterize flow rate Q , lumen area A and blood pressure P in the space-time domain through the following system of partial differential equations

$$\frac{\partial A}{\partial t} + \frac{\partial Q}{\partial x} = 0 \quad (1)$$

$$\frac{\partial Q}{\partial t} + \frac{\partial}{\partial x} \left(\frac{Q^2}{A} \right) = -\frac{A}{\rho} \frac{\partial P}{\partial x} - \frac{8\pi\mu}{\rho A} Q \quad (2)$$

where ρ and μ are blood density and viscosity, respectively. Poiseuille velocity profile has been assumed in (2). The behavior of the arterial wall is described by the following constitutive equation^{1,2}

$$P = P_o + \frac{\pi h R_o}{A} \left[E_E \varepsilon + E_C \varepsilon_r \ln(e^u + 1) + K_M \dot{\varepsilon} \right] \quad (3)$$

with $\varepsilon = \sqrt{\frac{A}{A_o}} - 1$ and so $\dot{\varepsilon} = \frac{\dot{A}}{2\sqrt{AA_o}}$, $u = \frac{\varepsilon - \varepsilon_o}{\varepsilon_r}$, where R , $A = \pi R^2$ (R_o , A_o are reference values at pressure $P_o = 1 \cdot 10^5 \text{ dyn/cm}^2$, which is of the order of the diastolic pressure), h is the arterial wall thickness, E_E , E_C and K_M are effective moduli for the elastin, collagen and viscoelastic components, respectively. Finally, ε_o and ε_r model the fiber recruitment through the localization and width of the distribution of the fiber strain activation. At bifurcations we consider the following coupling conditions

$$\sum_{i=1}^{N_T} Q_i = 0 \quad (4)$$

$$P_i + \frac{1}{2} \rho \left(\frac{Q_i}{A_i} \right)^2 = P_1 + \frac{1}{2} \rho \left(\frac{Q_1}{A_1} \right)^2 \quad i = 2, \dots, N_T \quad (5)$$

with N_T the number of arterial segments arriving at the junction. Terminal arterial segments are modeled as Windkessel elements

$$R_A R_B C \frac{dQ}{dt} = R_B C \frac{d}{dt} (P - P_T) + (P - P_T) - (R_A + R_B) Q \quad (6)$$

where P_T is a reference terminal pressure, C is the peripheral compliance and R_A and R_B are resistive elements.

Pertinent to the present study is the linear approximation of the pulse wave velocity (PWV) as given by the Moens-Korteweg equation

$$c = \sqrt{\frac{E_E h}{2\rho R_o}} \quad (7)$$

Numerical solution of the system of equations (1)-(2)-(3) with boundary conditions given by (6) is accomplished using the methodology described by Müller et al.³. In all cases, ten cardiac cycles are simulated to ensure that a periodic state is achieved.

Arteriolar beds

Arteriolar networks are generated by means of Constrained Constructive Optimization (CCO)^{4, 5}. The CCO technique generates a binary tree which can be set up by means of a given incoming flow rate and a given feeding vessel radius for a predefined perfusion volume. Figure 1 shows the CCO-generated arterial network within a typical spherical region. Color indicates vessel radii (unitary radius is considered at the inlet). The algorithm is stopped when the network reaches a predefined number of arterial segments (8000 in the figure). In practice, the algorithm is stopped for a given number of terminal vessels reaches a given value.

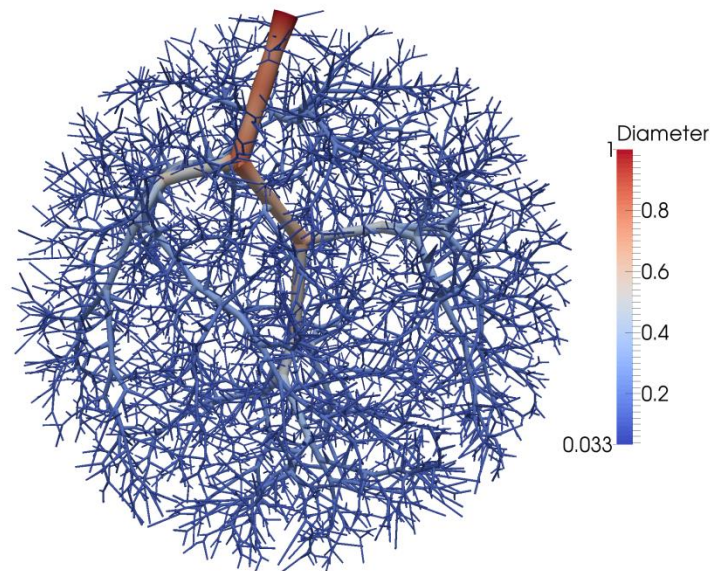


Figure S1: Arterial network automatically generated using CCO algorithm. A typical peripheral bed of spherical form containing 8000 arterial segments.

Arteriolar networks were constructed for two specific peripheral bed locations, namely the peripheral bed of the lenticulostriate artery and the peripheral bed of the posterior parietal branch of the middle cerebral artery. The data that characterizes these peripheral beds is reported in Table 1.

Peripheral beds					
Feeding artery	D	Q	V	n of terminal vessels	D_t (δD_t)
Lenticulostriate artery	0.582	0.0548	3.95	2000	45.4 (5.8)
Posterior parietal branch of middle cerebral artery	1.039	0.1230	18.51	10000	47.3 (6.5)

Table 1: Characterization of peripheral beds. Diameter of feeding artery ($D = 2R_o$, in mm), incoming flow rate (Q , in ml/s), perfused volume (V , in ml) and number of terminal vessels (n) in the resulting CCO-generated network. Also, for the terminal vessels in the arteriolar network, the mean diameter (D_t , in μm) and the standard deviation (δD_t , in μm) are reported.

The system of equations (1)-(5) governs the blood flow in the arteriolar networks. The setting of parameters follows that for arterial vessels except for the blood viscosity which is characterized by the following constitutive relation⁶

$$\mu = \left[1 + (\mu_{0.45}^* - 1) \frac{(1 - H_D)^C - 1}{(1 - 0.45)^C - 1} \left(\frac{D}{D - 1.1} \right)^2 \right] \left(\frac{D}{D - 1.1} \right)^2 \quad (8)$$

with

$$\mu_{0.45}^* = 6e^{-0.085D} + 3.2 - 2.44e^{-0.06D^{0.645}} \quad (9)$$

and

$$C = (0.8 + e^{-0.075D}) \left(-1 + \frac{1}{1 + 10^{-11} D^{12}} \right) + \frac{1}{1 + 10^{-11} D^{12}} \quad (10)$$

where $D = 2R_o$ is the vessel diameter and we have assumed that $H_D = 0.5$ is the value of the hematocrit.

At all terminal locations of the arteriolar networks a resistive terminal element (see equation (6) with $C = 0$) is considered. The value of these resistances is taken such that the flow rate is the same through each outlet and the pressure falls to the reference pressure P_T .

Normotensive scenario

The setting of the normotensive scenario follows the calibration criteria proposed by Blanco et al.¹. Relevant model parameters to the present study are the following

- h^N : wall thickness of the arterial vessels
- R_o^N : lumen radius of the arterial vessels
- R_w^N : total resistance of the network
- C_w^N : total compliance of the network

Hypertensive scenario

To model the hypertensive condition we consider the following modification of the model parameters (N and H denote normotensive and hypertensive cases)

- $h^H = 1.5h^N$: based on data previously reported⁷⁻¹⁰;
- $R_o^H = 0.9R_o^N$: based on data previously reported⁷⁻¹⁰;
- $R_w^H = 1.6R_w^N$: such that the mean arterial pressure is incremented approximately 50%, from the baseline healthy case, in central arteries;
- $C_w^H = 0.77C_w^N$: such that the peripheral compliance changes accordingly with the compliance of large vessels estimated through (7), that is the PWV results

$$c^H = \sqrt{\frac{E_E h^H}{2\rho R_o^H}} = \sqrt{\frac{1.5}{0.9}} \sqrt{\frac{E_E h^N}{2\rho R_o^N}}, \text{ and since } C_N^H \propto \frac{1}{c^H}, \text{ it results } C_N^H \propto 0.77 \frac{1}{c^N}.$$

For the arteriolar networks generated using CCO, the parameters were modified as detailed above.

These alterations are introduced in all vessels of the network, and are in compliance with the observed structural changes in arterial vessels for hypertensive animals (rats). The vessel distensibility (governed by E_E and E_C in the equations above) was not modified.

References

1. Blanco PJ, Watanabe SM, Passos MA, Lemos PA, Feijoo RA. An anatomically detailed arterial network model for one-dimensional computational hemodynamics. *IEEE Trans Biomed Eng.* 2015;62:736-753
2. Urquiza SA, Desimone H, Goni M, Introzzi A, Clara F. Prediction of human arterial pulse wave shape changes in aging and hypertension. In: H. Power RTH, Hosoda S. et al., ed. *Computer simulations in biomedicine*. Milan, Italy; 1995:131-138.
3. Müller LO, Blanco PJ, Watanabe SM, Feijoo RA. A high-order local time stepping finite volume solver for one-dimensional blood flow simulations: Application to the adan model. *International Journal for Numerical Methods in Biomedical Engineering.* . 2015;Submitted
4. Schreiner W. Computer generation of complex arterial tree models. *J Biomed Eng.* 1993;15:148-150

5. Blanco PJ, de Queiroz RA, Feijoo RA. A computational approach to generate concurrent arterial networks in vascular territories. *Int J Numer Method Biomed Eng.* 2013;29:601-614
6. Pries AR, Secomb TW, Gaehtgens P. Biophysical aspects of blood flow in the microvasculature. *Cardiovascular Research* 1996; 32:654-667.
7. Baumbach GL, Heistad DD. Remodeling of cerebral arterioles in chronic hypertension. *Hypertension.* 1989;13:968-972
8. Laurent S. Arterial wall hypertrophy and stiffness in essential hypertensive patients. *Hypertension.* 1995;26:355-362
9. New DI, Chesser AM, Thuraisingham RC, Yaqoob MM. Structural remodeling of resistance arteries in uremic hypertension. *Kidney Int.* 2004;65:1818-1825
10. Wolinsky H. Long-term effects of hypertension on the rat aortic wall and their relation to concurrent aging changes. Morphological and chemical studies. *Circ Res.* 1972;30:301-309